

# The Stannylphosphide Anion Reagent Sodium Bis(triphenylstannyl) Phosphide: Synthesis, Structural Characterization, and Reactions with Indium, Tin, and Gold Electrophiles

Christopher C. Cummins,<sup>\*,†</sup> Chao Huang,<sup>†,‡</sup> Tabitha J. Miller,<sup>†</sup> Markus W. Reintinger,<sup>†</sup> Julia M. Stauber,<sup>†</sup> Isabelle Tannou,<sup>†</sup> Daniel Tofan,<sup>†</sup> Abouzar Toubaei,<sup>§</sup> Alexandra Velian,<sup>\*,†</sup> and Gang Wu<sup>\*,§</sup>

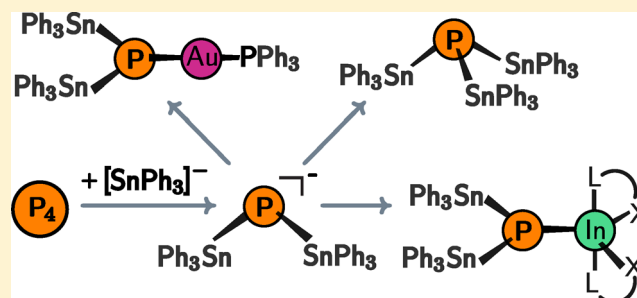
<sup>†</sup>Department of Chemistry, Massachusetts Institute of Technology, Cambridge, Massachusetts 02139-4307, United States

<sup>‡</sup>Department of Chemistry, College of Chemistry and Chemical Engineering, Xiamen University, Xiamen 361005, Fujian, China

<sup>§</sup>Department of Chemistry, Queen's University, Kingston, Ontario, Canada K7L3N6

## S Supporting Information

**ABSTRACT:** Treatment of  $P_4$  with in situ generated  $[Na][SnPh_3]$  leads to the formation of the sodium monophosphide  $[Na][P(SnPh_3)_2]$  and the Zintl salt  $[Na]_3[P_7]$ . The former was isolated in 46% yield as the crystalline salt  $[Na(\text{benzo-15-crown-5})][P(SnPh_3)_2]$  and used to prepare the homoleptic phosphine  $P(SnPh_3)_3$ , isolated in 67% yield, as well as the indium derivative  $(XL)_2InP(SnPh_3)_2$  ( $XL = S(CH_2)_2NMe_2$ ), isolated in 84% yield, and the gold complex  $(Ph_3P)AuP(SnPh_3)_2$ . The compounds  $[Na(\text{benzo-15-crown-5})][P(SnPh_3)_2]$ ,  $P(SnPh_3)_3$ ,  $(XL)_2InP(SnPh_3)_2$ , and  $(Ph_3P)AuP(SnPh_3)_2$  were characterized using multinuclear NMR spectroscopy and X-ray crystallography. The bonding in  $(Ph_3P)AuP(SnPh_3)_2$  was dissected using natural bond orbital (NBO) methods, in response to the observation from the X-ray crystal structure that the dative  $P \rightarrow Au$  bond is slightly shorter than the shared electron-pair  $P-Au$  bond. The bonding in  $(XL)_2InP(SnPh_3)_2$  was also interrogated using  $^{31}P$  and  $^{13}C$  solid-state NMR and computational methods. Co-product  $[Na]_3[P_7]$  was isolated in 57% yield as the stannyl heptaphosphide  $P_7(SnPh_3)_3$ , following salt metathesis with  $ClSnPh_3$ . Additionally, we report that treatment of  $P_4$  with sodium naphthalenide in dimethoxyethane at 22 °C is a convenient and selective method for the independent synthesis of Zintl ion  $[Na]_3[P_7]$ . The latter was isolated as the silylated heptaphosphide  $P_7(SiMe_3)_3$ , in 67% yield, or as the stannyl heptaphosphide  $P_7(SnPh_3)_3$  in 65% yield by salt metathesis with  $ClSiMe_3$  or  $ClSnPh_3$ , respectively.



## 1. INTRODUCTION

Simple phosphide reagents have diverse applications in inorganic and materials synthesis, and unique among them are salts of the  $[P(SiMe_3)_2]^-$  anion in terms of being able to generate new P-element bonds by salt elimination as well as by production of  $XSiMe_3$  species.<sup>1–6</sup> For example, phosphalkynes were prepared by treatment of the monophosphide  $Li[P(SiMe_3)_2]$  with acyl chlorides;<sup>1</sup> gallium mono and diphosphides ( $^tBu$ -DAB)(X)GaP(SiMe<sub>3</sub>)<sub>2</sub>, (DAB = [ $^tBuNC(H)$ ]<sub>2</sub>, X = I, P(SiMe<sub>3</sub>)<sub>2</sub>) were prepared by treatment of [ $^tBu$ -DAB]GaI<sub>2</sub> with  $Li[P(SiMe_3)_2]$ ,<sup>3</sup> and the disilylphosphido complex  $Cp^*-(CO)_2(NO)MnP(SiMe_3)_2$  was obtained from the reaction of  $[Cp^*-(CO)_2(NO)Mn]BF_4$  with  $LiP(SiMe_3)_2$ .<sup>2</sup> Despite this considerable versatility, there is a synthetic barrier to be overcome in obtaining alkali metal salts  $M[P(SiMe_3)_2]$ ; for example,  $Li[P(SiMe_3)_2]$  has been obtained by methylindium reaction with  $P(SiMe_3)_3$ , which in turn must be either synthesized (typically by initial treatment of white phosphorus with hazardous Na/K alloy in a procedure that generates pyrophoric waste) or purchased at high cost.<sup>7</sup> Accordingly, we wondered if it might be possible to prepare such a reagent in

one operation, directly from white phosphorus and using a more streamlined protocol. For the present investigation we settled on sodium naphthalenide as the reducing agent, as this is conveniently generated in a nitrogen-atmosphere glovebox upon stirring a mixture of sodium and naphthalene at ambient temperature in tetrahydrofuran (THF).<sup>8</sup> We were pleased to discover that subsequent addition of  $ClSnPh_3$  (to generate  $[Na][SnPh_3]$ ) followed by  $P_4$  delivers the new phosphide anion  $[P(SnPh_3)_2]^-$ , which was isolated in 46% yield as its  $[Na(\text{benzo-15-crown-5})]^+$  salt and fully characterized including an X-ray diffraction study (see Figure 1). The optimized reaction conditions also give rise to formation of the well-known  $P_7^{3-}$  anion, which can be converted in situ to  $P_7R_3$  ( $R = SiMe_3, SnPh_3$ ) for isolation if desired (see Scheme 1). As expected, treatment of  $[P(SnPh_3)_2]^-$  salts with  $ClSnPh_3$  produces  $P(SnPh_3)_3$ , for which an X-ray structural study is provided (see Figure 2). Further illustrating the potential utility of the new stannylphosphide reagent, reaction with  $(XL)_2InI$

Received: December 31, 2013

Published: March 12, 2014

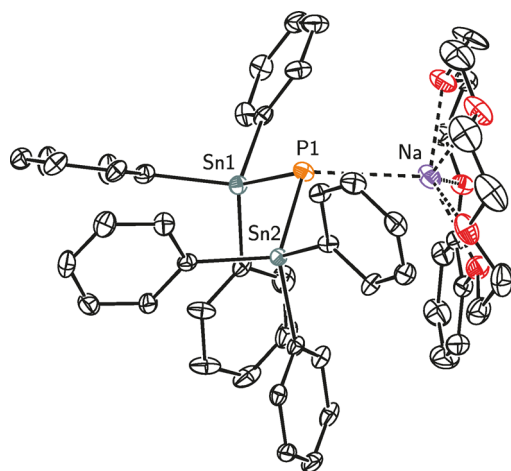
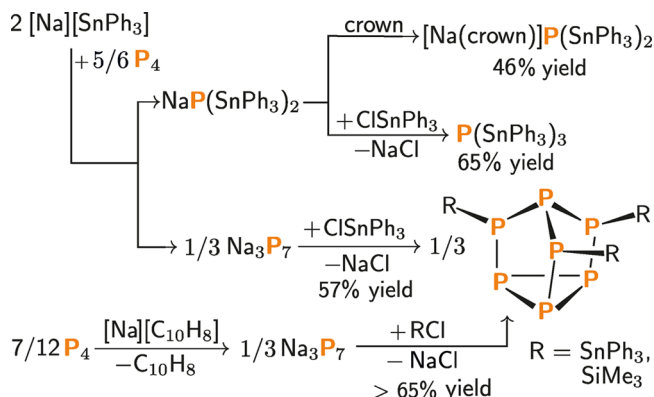


**Figure 1.** Solid-state molecular structure of  $[\text{Na}(\text{benzo-15-crown-5})][\text{P}(\text{SnPh}_3)_2]$  with ellipsoids at the 50% probability level and rendered using PLATON.<sup>11</sup> The other  $[\text{Na}(\text{benzo-15-crown-5})][\text{P}(\text{SnPh}_3)_2]$  molecule present in the asymmetric unit and hydrogen atoms are omitted for clarity. Selected interatomic distances [Å] and angles [deg]: P1–Na1 2.891(2), P1–Sn1 2.439(1), P1–Sn2 2.438(1), P2–Sn3 2.438(2), P2–Sn4 2.442(2), P2–Na2 2.927(2), Sn1–P1–Sn2 101.07(5), Sn2–P1–Na1 108.56(6), Sn1–P1–Na1 108.63(6).

### Scheme 1<sup>a</sup>



<sup>a</sup>A series of tetrel phosphides were obtained by reaction of white phosphorus with either the stannyl salt  $[\text{Na}][\text{SnPh}_3]$  or sodium naphthalene,  $[\text{Na}][\text{C}_{10}\text{H}_8]$ . The corresponding phosphides were obtained via salt metathesis with  $\text{RCl}$ , where  $\text{R} = \text{SiMe}_3, \text{SnPh}_3$  (crown = benzo-15-crown-5).

$(\text{XL})_2\text{InP}(\text{SnPh}_3)_2$ <sup>9,10</sup> was found efficiently to furnish a terminal indium phosphanide species,  $(\text{XL})_2\text{In}-\text{P}(\text{SnPh}_3)_2$ , featuring an unsupported indium- $\text{PR}_2$  linkage. Characterization data provided for the latter stem from both a crystallographic structure determination and interrogation by solid-state NMR methods (see Table 1). Additionally, the gold complex  $(\text{Ph}_3\text{P})\text{AuP}(\text{SnPh}_3)_2$  could be prepared in the salt elimination reaction of  $[\text{Na}(\text{benzo-15-crown-5})][\text{P}(\text{SnPh}_3)_2]$  with  $(\text{Ph}_3\text{P})\text{-AuCl}$ .

## 2. EXPERIMENTAL SECTION

**General Information.** All manipulations were performed in a Vacuum Atmospheres model MO-40 M glovebox under an inert atmosphere of purified  $\text{N}_2$ . All solvents were obtained anhydrous and oxygen-free by bubble degassing ( $\text{N}_2$ ) and purification through columns of alumina and Q5 using a Glass Contours Solvent Purification System built by SG Water.  $(\text{XL})_2\text{InI}$  was prepared

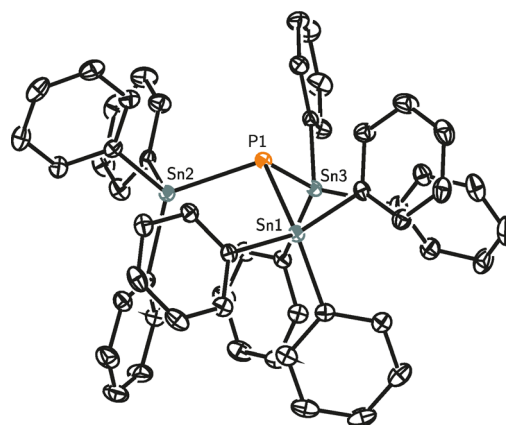


**Figure 2.** Solid-state molecular structure of  $\text{P}(\text{SnPh}_3)_3$  with ellipsoids at the 50% probability level and rendered using PLATON.<sup>11</sup> Hydrogen atoms and the solvent molecule are omitted for clarity. Selected interatomic distances [Å] and angles [deg]: P1–Sn1 2.5068(6), P1–Sn2 2.5082(6), P1–Sn3 2.5108(6), Sn1–P1–Sn3 104.25(2), Sn1–P1–Sn2 103.04(2), Sn2–P1–Sn3 102.26(2).

according to the literature procedure.<sup>10</sup> White phosphorus was acquired from ThermPhos International BV,  $\text{Ph}_3\text{SnCl}$  95% was purchased from Alfa Aesar,  $(\text{Ph}_3\text{P})\text{AuCl}$  was purchased from Strem Chemicals, while all other reagents were purchased from Aldrich and were used without further purification. Deuterated solvents were purchased from Cambridge Isotope Laboratories. Benzene- $d_6$  was degassed and stored over molecular sieves (4 Å beads, 8–12 mesh) for at least 2 d prior to use. Celite 435 (EM Science) was dried by heating above 200 °C under dynamic vacuum for at least 24 h prior to use. All glassware was oven-dried for at least 3 h prior to use, at temperatures greater than 150 °C. NMR spectra were obtained on Bruker Avance 400 instruments equipped with Magnex Scientific superconducting magnets.  $^1\text{H}$  and  $^{13}\text{C}\{^1\text{H}\}$  NMR spectra were referenced to residual solvent proton resonances in benzene- $d_6$  ( $^1\text{H} = 7.16$  ppm,  $^{13}\text{C} = 128.06$  ppm, respectively); spectra were referenced externally to 85%  $\text{H}_3\text{PO}_4$  (0 ppm).  $^{119}\text{Sn}$  NMR spectra were referenced externally to 5%  $\text{SnMe}_4$  in  $\text{CH}_2\text{Cl}_2$  (0 ppm). Elemental combustion analyses were performed by Intertek USA, Inc., by Complete Analysis Laboratories Inc., or by Robertson Microлит Laboratories. Solid-state  $^{31}\text{P}$  and  $^{13}\text{C}$  NMR spectra were acquired under the cross-polarization (CP) magic-angle spinning (MAS) condition on a Bruker Avance-600 NMR spectrometer (14.0 T) operating at the  $^1\text{H}$ ,  $^{31}\text{P}$ , and  $^{13}\text{C}$  Larmor frequencies of 600.17, 242.95, and 150.93 MHz, respectively. High-power  $^1\text{H}$  decoupling was applied during data acquisition. Solid  $(\text{XL})_2\text{InP}(\text{SnPh}_3)_2$  was packed into a  $\text{ZrO}_2$  rotor (4 mm o.d.) inside a glovebox. A 4 mm Bruker H/X MAS probe was used with a sample spinning frequency of 14.5 kHz. Typically, relaxation delays of 2–5 s were employed. All  $^{31}\text{P}$  and  $^{13}\text{C}$  chemical shifts were referenced to the signals of 85%  $\text{H}_3\text{PO}_4$  (aq) and tetramethylsilane, respectively, using solid  $\text{NH}_4\text{H}_2\text{PO}_4$  and glycine as secondary referencing samples. Spectral simulations were performed using WSolid1.<sup>12</sup>

**Crude Triphenylstannylsodium ( $[\text{Na}][\text{SnPh}_3]$ ).** This was synthesized using a slightly modified literature procedure.<sup>13</sup> THF (10 mL) was added to a mixture of sodium metal (0.138 g, 6.00 mmol, 2.00 equiv) and naphthalene (0.768 g, 5.99 mmol, 2.00 equiv). The reaction mixture was stirred vigorously for at least 5 h, until all the sodium metal was consumed. The resulting dark green reaction mixture was added dropwise to a solution of  $\text{Ph}_3\text{SnCl}$  (1.156 g, 3.00 mmol, 1.00 equiv) in THF (20 mL) under vigorous stirring, resulting in an orange-brown mixture.  $^{119}\text{Sn}$  NMR analysis of an aliquot showed a single broad peak at  $-105$  ppm corresponding to the  $[\text{Na}][\text{SnPh}_3]$ . The volatile materials from the reaction mixture were removed under reduced pressure, and the resulting oily residue was stirred in *n*-hexane (10 mL), then again brought to constant mass under reduced pressure. The orange-brown powder obtained this way was slurried in *n*-hexane (20 mL), and the supernatant was decanted away. The precipitated off-

white powder containing the  $[\text{Na}][\text{SnPh}_3]$  salt was used in the next steps without any further purification, under the assumption that the transformation had been quantitative.

**Reaction of  $\text{P}_4$  with  $[\text{Na}][\text{SnPh}_3]$ .** A 100 mL round-bottom flask was charged with THF (10 mL),  $\text{Et}_2\text{O}$  (30 mL), crude  $[\text{Na}][\text{SnPh}_3]$  (ca. 3 mmol, 2 equiv) and a Teflon-coated stir bar. To this mixture, a solution of  $\text{P}_4$  (0.186 g, 1.50 mmol, 1.20 equiv) in toluene (15 mL) was added dropwise under vigorous stirring. The color of the reaction mixture changed to vivid orange, and an orange-red precipitate formed. The resulting slurry was filtered through a pad of Celite in a sintered glass frit. The orange filter cake containing the  $[\text{Na}]_3[\text{P}_7]$  was set aside and worked up separately, as described below.

**$[\text{Na}(\text{benzo-15-crown-5})][\text{P}(\text{SnPh}_3)_2]$ .** To the orange filtrate obtained as described in the previous section was added, in one portion, benzo-15-crown-5 (0.402 g, 1.50 mmol, 1.00 equiv), effecting the immediate precipitation of red solids. The reaction mixture was subjected to filtration through a fritted filter funnel, and the resulting filtrate was stirred for another 30 min before the volatile materials were removed under reduced pressure. The residue was slurried in toluene (5 mL), then allowed to settle, and the pale yellow supernatant was decanted by pipet and discarded. The oily solids so obtained were placed under vacuum before being slurried in  $\text{Et}_2\text{O}$  (8 mL) for 1 h, effecting the formation of a powder, which was then allowed to settle. The supernatant was again separated by pipet and discarded, and all volatile materials were removed from the resulting yellow powder under reduced pressure. Next, this material was extracted three times with toluene ( $3 \times 5$  mL), to remove traces of  $\text{P}_7(\text{SnPh}_3)_3$ , and then six times with  $\text{Et}_2\text{O}$  ( $6 \times 5$  mL) to remove  $\text{P}(\text{SnPh}_3)_3$ . The residue, brought to constant mass under reduced pressure, was deemed spectroscopically pure  $[\text{Na}(\text{benzo-15-crown-5})][\text{P}(\text{SnPh}_3)_2]$  (713 mg, 0.69 mmol, 46%).  $^1\text{H}$  NMR (benzene- $d_6$ , 20 °C, 400 MHz)  $\delta$ : 3.01 (m, 4 H), 3.08 (m, 4 H), 3.16 (m, 4 H), 3.26 (m, 4 H), 6.41 (m, 2 H), 6.78 (m, 2 H), 7.10 (m, 18 H), 7.82 (m,  $^3J_{\text{SnH}} = 50$  Hz, 12 H) ppm.  $^{13}\text{C}\{^1\text{H}\}$  NMR (benzene- $d_6$ , 20 °C, 100.6 MHz)  $\delta$ : 66.76 ( $\text{CH}_2$ ), 67.53 ( $\text{CH}_2$ ), 68.82 ( $\text{CH}_2$ ), 69.11 ( $\text{CH}_2$ ), 112.83, 121.98, 127.37, 127.87, 137.74 ( $^2J_{\text{SnC}} = 38$  Hz,  $\text{SnC}_6\text{H}_5$ ), 147.13 ( $\text{SnC}_6\text{H}_5$ ), 147.68 (d,  $^2J_{\text{PC}} = 3$  Hz,  $\text{SnC}_6\text{H}_5$ ) ppm.  $^{31}\text{P}\{^1\text{H}\}$  NMR (benzene- $d_6$ , 20 °C, 161.9 MHz)  $\delta$ : -367.2 (s,  $^1J_{119\text{SnP}} = 1395$  Hz,  $^1J_{117\text{SnP}} = 1329$  Hz) ppm.  $^{119}\text{Sn}$  NMR (149.2 MHz, benzene- $d_6$ )  $\delta$ : -11.0 (s,  $^1J_{119\text{SnP}} = 1395$  Hz) ppm. Elemental analysis (%) found (calculated) for  $\text{C}_{50}\text{H}_{50}\text{NaO}_5\text{P}_2\text{Sn}_2$ : C 58.60(58.74), H 4.43(4.93), and P 3.13(3.03). Melting point: 185–186 °C.

**$\text{P}_7(\text{SnPh}_3)_3$  (Method A).** The orange filter cake obtained as described above and contained on a bed of Celite in a fritted glass filter funnel was washed with THF (15 mL), and the resulting orange filtrate containing  $[\text{Na}]_3[\text{P}_7]$  ( $^{31}\text{P}$  NMR  $\delta = -120$  ppm) was collected.<sup>14</sup> To this mixture, a solution of  $\text{ClSnPh}_3$  (0.578 g, 1.50 mmol, 3.00 equiv with respect to the theoretical amount of  $[\text{P}_7]^{-3}$  anion formed in the reaction, based on the equation in Scheme 1) in THF (8 mL) was added dropwise, effecting a color change from orange to brown. The reaction mixture was brought to constant mass under reduced pressure, and the resulting brown residue was suspended in a mixture of  $n$ -hexane (10 mL) and  $\text{Et}_2\text{O}$  (20 mL). The suspension was subjected to filtration through a fritted filter funnel, and the volatile materials were removed from the resulting filtrate under reduced pressure. The obtained residue was suspended in a mixture of  $\text{Et}_2\text{O}$  (10 mL) and toluene (10 mL) and subjected again to filtration through a pad of Celite. The filtrate was brought to constant mass under reduced pressure, yielding spectroscopically pure  $\text{P}_7(\text{SnPh}_3)_3$  as a yellow powder (0.341 g, 0.285 mmol, 57% yield). The NMR spectra ( $^1\text{H}$ ,  $^{31}\text{P}$ ) were consistent with reported values.<sup>15</sup>

**$\text{P}(\text{SnPh}_3)_3$ .** A 100 mL round-bottom flask was charged with THF (10 mL),  $\text{Et}_2\text{O}$  (30 mL), crude  $[\text{Na}][\text{SnPh}_3]$  (ca. 3 mmol, 2 equiv), and a Teflon-coated stir bar. A solution of  $\text{P}_4$  (0.186 g, 1.50 mmol, 1.20 equiv) in toluene (15 mL) was added dropwise under vigorous stirring as the color of the reaction mixture changed to vivid orange and an orange-red precipitate formed. The resulting slurry was subjected to filtration through a pad of Celite in a fritted filter funnel. To the orange filtrate containing  $[\text{Na}][\text{P}(\text{SnPh}_3)_2]$  salt was added dropwise a slurry of  $\text{ClSnPh}_3$  (0.578 g, 1.50 mmol, 1.00 equiv) in THF

(10 mL), during which addition the reaction mixture turned colorless. The volatile materials were then removed under reduced pressure, and the resulting white residue was washed with  $n$ -hexane (20 mL) and suspended in  $\text{Et}_2\text{O}$  (20 mL). This suspension was subjected to filtration through a pad of Celite in a fritted filter funnel, and the filter cake was washed with additional toluene (20 mL). The combined filtrate was concentrated under reduced pressure and brought to constant mass to afford colorless solids of spectroscopically pure  $\text{P}(\text{SnPh}_3)_3$  (0.98 g, 0.97 mmol, 65% yield). Analytically pure  $\text{P}(\text{SnPh}_3)_3$  was obtained by collecting the crystals formed upon cooling a saturated solution of the spectroscopically pure material in  $\text{Et}_2\text{O}$ , at -35 °C.  $^1\text{H}$  NMR (benzene- $d_6$ , 20 °C, 400 MHz)  $\delta$ : 6.98 (m, 18 H), 7.09 (9 H), 7.24 (m,  $^3J_{119\text{SnH}} = 58$  Hz,  $^3J_{117\text{SnH}} = 44$  Hz, 18 H) ppm.  $^{13}\text{C}\{^1\text{H}\}$  NMR (benzene- $d_6$ , 20 °C, 100.6 MHz)  $\delta$ : 128.77, 129.06, 137.62 ( $^2J_{\text{SnC}} = 5$  Hz), 140.62 (dt,  $^2J_{\text{PC}} = 40$  Hz) ppm.  $^{31}\text{P}\{^1\text{H}\}$  NMR (benzene- $d_6$ , 20 °C, 161.9 MHz)  $\delta$ : -325.2 (s,  $^1J_{119\text{SnP}} = 886$  Hz,  $^1J_{117\text{SnP}} = 855$  Hz) ppm.  $^{119}\text{Sn}$  NMR (149.2 MHz, benzene- $d_6$ )  $\delta$ : -69.2 (d,  $^1J_{119\text{SnP}} = 886$  Hz) ppm. Elemental analysis (%) found (calculated) for  $\text{C}_{54}\text{H}_{45}\text{P}_3\text{Sn}_3$ : C 60.14(60.00), H 4.09(4.20), P 2.79(2.87). Melting point: 208–210 °C.

**$(\text{XL})_2\text{InP}(\text{SnPh}_3)_2$  ( $\text{XL} = \text{S}(\text{CH}_2)_2\text{NMe}_2$ ).** Cold toluene (-35 °C, 5 mL) was added to a 100 mL round-bottom flask containing solid  $(\text{XL})_2\text{InI}$  (90 mg, 0.20 mmol, 1.00 equiv) and  $[\text{Na}(\text{benzo-15-crown-5})][\text{P}(\text{SnPh}_3)_2]$  (0.204 g, 0.20 mmol, 1.00 equiv). The reaction mixture was stirred for 20 min before adding more cold toluene (5 mL). After 1.5 h of stirring at 22 °C, the reaction mixture was filtered through a pad of Celite in a fritted filter funnel. The volatile materials were removed from the colorless filtrate under reduced pressure, resulting in spectroscopically pure  $(\text{XL})_2\text{InP}(\text{SnPh}_3)_2$  as a white powder (176 mg, 0.167 mmol, 84% yield).  $^1\text{H}$  NMR (benzene- $d_6$ , 20 °C, 400 MHz)  $\delta$ : 1.86 (s, 12 H), 1.98 (broad s, 4 H), 2.41 (broad s, 4 H), 7.12 (m, 18 H), 7.70 (m, 12 H) ppm.  $^{13}\text{C}\{^1\text{H}\}$  NMR (benzene- $d_6$ , 20 °C, 100.6 MHz)  $\delta$ : 24.62 ( $\text{CH}_3$ ), 45.36 ( $\text{CH}_2$ ), 61.35 ( $\text{CH}_2$ ), 128.67 ( $\text{SnC}_6\text{H}_5$ ), 128.88 ( $\text{SnC}_6\text{H}_5$ ), 137.94 ( $^2J_{\text{SnC}} = 40$  Hz,  $\text{SnC}_6\text{H}_5$ ), 142.6 ppm ( $\text{SnC}_6\text{H}_5$ ).  $^{31}\text{P}\{^1\text{H}\}$  NMR (benzene- $d_6$ , 20 °C, 161.9 MHz)  $\delta$ : -309.9 (s,  $^1J_{119\text{SnP}} = 990$  Hz,  $^1J_{117\text{SnP}} = 950$  Hz) ppm.  $^{119}\text{Sn}$  NMR (149.2 MHz, benzene- $d_6$ )  $\delta$ : -65.9 (d,  $^1J_{119\text{SnP}} = 990$  Hz) ppm. Elemental analysis (%) found (calculated) for  $\text{C}_{44}\text{H}_{50}\text{InN}_2\text{S}_2\text{Sn}_2\text{P}$ : C 50.08(50.13), H 4.69(4.78), N 2.53(2.66), P 2.79(2.94)

**$\text{P}_7(\text{SiMe}_3)_3$ .** To a solution of naphthalene (3.540 g, 27.60 mmol, 3.00 equiv) in dimethoxyethane (DME) (20 mL) were added small pieces of freshly cut sodium metal (0.635 g, 27.60 mmol, 3.00 equiv). The reaction mixture was vigorously stirred for 8 h or longer, until all the sodium metal was consumed. The sodium naphthalenide solution was then added to a slurry of  $\text{P}_4$  (2.000 g, 16.14 mmol, 1.75 equiv) in DME (30 mL), in a round-bottom flask covered in Al foil. The reaction mixture was stirred for 8 h, at which point  $\text{ClSiMe}_3$  (3.000 g, 27.60 mmol, 3.00 equiv) was added dropwise. The resulting orange-red slurry was stirred for 2 h, then brought to constant mass under reduced pressure. The dark red solids were transferred to the bottom of a sublimation apparatus, which was then evacuated. The apparatus was then removed from the glovebox and set up for sublimation in an oil bath preheated to 60 °C, with the circulating water at 6 °C. After approximately 7 h when all the naphthalene had been removed by sublimation, the apparatus was returned to the glovebox, where dark red solids at the bottom of the sublimation apparatus were slurried in  $n$ -pentane (100 mL) and then subjected to filtration through a Celite pad contained within a fritted filter funnel. The Celite pad was washed with additional  $n$ -pentane until the filtrate ran colorless. The combined yellow filtrate was concentrated before being set at -35 °C for crystallization. Yellow crystals of  $\text{P}_7(\text{SiMe}_3)_3$  formed overnight and were collected by filtration in several crops (2.700 g, 6.10 mmol, 67% yield). The observed  $^1\text{H}$  and  $^{31}\text{P}$  NMR signals were consistent with reported values.<sup>16</sup>

**$\text{P}_7(\text{SnPh}_3)_3$  (Method B).** To a solution of naphthalene (0.897 g, 7.00 mmol, 3.00 equiv) in DME (7 mL) were added small pieces of freshly cut sodium metal (0.161 g, 7.00 mmol, 3.00 equiv). The reaction mixture was vigorously stirred for 5 h or longer, until all the sodium metal was consumed. The sodium naphthalenide solution was then added to a slurry of  $\text{P}_4$  (0.500 g, 4.04 mmol, 1.73 equiv) in DME

(5 mL), with the aid of additional DME (5 mL), and the reaction flask was protected from light by covering in Al foil. The reaction mixture was stirred for 10 h, at which point solid  $\text{ClSnPh}_3$  (2.700 g, 7.00 mmol, 1.73 equiv) was added in one portion. The orange-red slurry was stirred for 4 h and then brought to constant mass under reduced pressure. The yellow-orange solids were transferred to the bottom of a sublimation apparatus, which was then evacuated. The apparatus was then removed from the glovebox and set up for sublimation in an oil bath preheated to 60 °C, with the circulating water at 6 °C. After approximately 8 h, when all the naphthalene had been removed by sublimation, the apparatus was returned to the glovebox, where the yellow solids at the bottom of the sublimation apparatus were slurried in *n*-pentane (100 mL) and then subjected to filtration through a Celite pad contained within a fritted filter funnel. The Celite pad was washed with additional *n*-pentane until the filtrate ran colorless. The volatile materials were then removed from the combined filtrate under reduced pressure, resulting in an orange-yellow residue, which was slurried in *n*-hexane (5 mL), then brought back to constant mass. The collected yellow powder was identified as pure  $\text{P}_7(\text{SnPh}_3)_3$  (1.982 g, 1.56 mmol, 65%) using  $^1\text{H}$  and  $^{31}\text{P}$  NMR spectroscopy.<sup>15</sup>

**$(\text{Ph}_3\text{P})\text{AuP}(\text{SnPh}_3)_2$ .** A solution of  $(\text{Ph}_3\text{P})\text{AuCl}$  (243 mg, 0.49 mmol, 1 equiv) in toluene (20 mL) was added dropwise, at room temperature, to a slurry of  $[\text{Na}(\text{benzo-15-crown-5})][\text{P}(\text{SnPh}_3)_2]$  (500 mg, 0.49 mmol, 1 equiv) in toluene (20 mL). The reaction mixture was stirred for 30 min and then was subjected to filtration through a pad of Celite. All volatile materials were removed under reduced pressure from the yellow filtrate. The resulting yellow powder was washed with  $\text{Et}_2\text{O}$  ( $2 \times 5$  mL and  $1 \times 10$  mL) and was then brought to constant mass under reduced pressure to afford 322 mg of a beige powder.  $^{31}\text{P}$  NMR spectroscopy confirmed the composition of the material to be a mixture of free  $\text{PPh}_3$  (ca. 7%) and  $(\text{Ph}_3\text{P})\text{AuP}(\text{SnPh}_3)_2$  (estimated 0.27 mmol, 55%). Further purification efforts, including recrystallization and  $\text{Et}_2\text{O}$  extraction of the  $\text{PPh}_3$  impurity, were unsuccessful. Satisfactory combustion elemental analysis was not obtained for this compound.  $^1\text{H}$  NMR (benzene- $d_6$ , 20 °C, 400 MHz)  $\delta$ : 6.92 (m, 8 H), 6.99 (m, 16 H), 7.09 (m, 9 H) ppm.  $^{13}\text{C}\{^1\text{H}\}$  NMR (benzene- $d_6$ , 20 °C, 100.6 MHz)  $\delta$ : 128.47, 128.71, 129.19, 129.30, 131.09, 134.46, 134.60, 137.60 ppm.  $^{31}\text{P}\{^1\text{H}\}$  NMR (benzene- $d_6$ , 20 °C, 161.9 MHz)  $\delta$ : -303.9 (d,  $^2J_{\text{PP}} = 78$  Hz,  $^1J_{119\text{SnP}} = 524$  Hz), 46.68 (d,  $^2J_{\text{PP}} = 78$  Hz,  $^3J_{119\text{SnP}} = 27$  Hz) ppm.  $^{119}\text{Sn}$  NMR (149.2 MHz, benzene- $d_6$ )  $\delta$ : -44.10 (dd,  $^1J_{119\text{SnP}} = 1046$  Hz,  $^3J_{119\text{SnP}} = 55$  Hz) ppm.

**Computational Methods.** NMR parameters were computed using the Amsterdam Density Functional (ADF) software package.<sup>17</sup> The Vosko–Wilk–Nusair (VWN) exchange–correlation functional<sup>18</sup> was used for the local density approximation (LDA), and the Perdew–Burke–Ernzerhof (PBE) exchange–correlation functional<sup>19</sup> was applied for the generalized gradient approximation (GGA). Standard Slater-type-orbital (STO) basis sets with triple- $\zeta$  quality plus polarization functions (TZ2P) were used for all the atoms. The spin–orbital relativistic effect was incorporated via the zero-order regular approximation (ZORA).<sup>20</sup> The crystallographically determined molecular structure of  $(\text{XL})_2\text{InP}(\text{SnPh}_3)_2$  was used directly in the computations. The  $^{31}\text{P}$  chemical shift ( $\delta$ ) was converted from the computed shielding constant ( $\sigma$ ) using the absolute  $^{31}\text{P}$  shielding scale:<sup>21</sup>  $\delta = 328.35 - \sigma$ . All quantum-chemical calculations pertaining to the analysis of  $(\text{XL})_2\text{InP}(\text{SnPh}_3)_2$  were performed at the High Performance Computing Virtual Laboratory (HPCVL) at Queen's University.

The calculations pertaining to the gold model complex  $\text{H}_3\text{P–Au–PH}_2$ , built using Molden,<sup>22</sup> were performed at the second-order Møller–Plesset perturbation theory (MP2) level,<sup>23</sup> as well as at the B3LYP level, and were carried out using the ORCA 3.0.1 quantum chemistry program package.<sup>24</sup> The LDA functional employed was LYP<sup>25</sup> or PW-LDA,<sup>26</sup> while the GGA part was handled using the functionals of Becke and Perdew (BP86 or BLYP).<sup>27</sup> The TZVPP basis set was used for all atoms,<sup>28</sup> the spin–orbital relativistic effect was incorporated via the zero-order approximation (ZORA),<sup>20</sup> and tight self-consistent field convergence criteria (provided by ORCA) were employed. The nature of the dative  $\text{P} \rightarrow \text{Au}$  and shared electron

pair  $\text{P–Au}$  bonds were analyzed with the aid of natural bond order (NBO)<sup>29</sup> and natural resonance theory (NRT) analysis.<sup>30</sup>

**X-ray Diffraction Studies.** Diffraction-quality, light yellow crystals of  $[\text{Na}(\text{benzo-15-crown-5})][\text{P}(\text{SnPh}_3)_2]$  were obtained by vapor diffusion of *n*-pentane into a concentrated solution of the salt in THF. Colorless crystals of  $\text{P}(\text{SnPh}_3)_3$  were grown upon cooling a warm solution in  $\text{Et}_2\text{O}/n$ -hexane (1:1) to 22 °C. X-ray quality crystals of  $(\text{Ph}_3\text{P})\text{AuP}(\text{SnPh}_3)_2$  were grown at room temperature by vapor diffusion of *n*-pentane into a concentrated solution of the gold phosphide in toluene. Low-temperature (100 K) data were collected on a Siemens Platform three-circle diffractometer coupled to a Bruker-AXS Smart Apex CCD detector with graphite-monochromated  $\text{Mo K}\alpha$  radiation ( $\lambda = 0.71073$  Å) and on a Bruker-AXS X8 Kappa Duo diffractometer coupled to a Smart Apex2 charge-coupled device (CCD) detector with  $\text{Mo K}\alpha$  radiation ( $\varphi$ - and  $\omega$ -scans). A semiempirical absorption correction was applied to the diffraction data using SADABS.<sup>31</sup> All structures were solved by direct or Patterson methods using SHELXS<sup>32,33</sup> and refined against  $F^2$  on all data by full-matrix least-squares with SHELXL-97.<sup>33,34</sup> All non-hydrogen atoms were refined anisotropically. All hydrogen atoms were included in the model at geometrically calculated positions and refined using a riding model. The isotropic displacement parameters of all hydrogen atoms were fixed to 1.2 times the  $U_{\text{eq}}$  value of the atoms they are linked to (1.5 times for methyl groups).<sup>35</sup> Descriptions of the individual refinements follow below. Details of the data quality and a summary of the residual values of the refinements for all structures are provided in Supporting Information, Table S.1 and in the form of .cif files available from the CCDC under the deposition numbers 943071, 943072, 974655, and 974656.<sup>36</sup>

The sodium phosphide  $[\text{Na}(\text{benzo-15-crown-5})][\text{P}(\text{SnPh}_3)_2]$  crystallized in the monoclinic space group  $P2_1$  with two molecules in the asymmetric unit. One of the twelve phenyl rings and one of the two phenylene groups were each disordered over two positions. The phosphide  $\text{P}(\text{SnPh}_3)_3$  crystallized in the orthorhombic space group  $P2_1/n$ , with an asymmetric unit containing two molecules of compound and one molecule of diethyl ether, which was disordered over two positions. The two occupancies of each disordered position were refined freely, and their sums were restrained to unity. The indium phosphide  $(\text{XL})_2\text{InP}(\text{SnPh}_3)_2$  crystallized in the monoclinic space group  $P2_1$ , with an asymmetric unit containing one molecule of compound and one molecule of toluene, which was disordered over the inversion center. Additionally, one of the six phenyl rings was disordered over two positions, and the two  $\text{S}(\text{CH}_2)_2\text{NMe}_2$  arms on the indium atom were disordered over a total of five positions.

The gold phosphide  $(\text{Ph}_3\text{P})\text{AuP}(\text{SnPh}_3)_2$  crystallized in the triclinic space group  $P\bar{1}$  with four molecules per asymmetric unit. Two phenyl rings ( $\text{SnPh}_3$ ) were disordered over two positions. Refinement of the structure against a smaller unit cell, which contained only two molecules per asymmetric unit, led to the generalized disorder of the phenyl groups and an unsatisfying solution. The occupancies of each disordered position were refined freely, and their sums were restrained to unity. Similarity restraints on 1–2 and 1–3 distances and displacement parameters, as well as rigid bond restraints for anisotropic displacement parameters, were applied to the disordered fragments.

### 3. RESULTS AND DISCUSSION

**Synthesis and Structure.** Treatment of a 1:3 THF/ $\text{Et}_2\text{O}$  solution of the in situ-generated stannyl anion  $[\text{SnPh}_3]^-$  with a solution of  $\text{P}_4$  in toluene at 22 °C led to the formation of monophosphide  $[\text{Na}][\text{P}(\text{SnPh}_3)_2]$  and the Zintl ion coproduct  $[\text{Na}]_3[\text{P}_7]$ .<sup>37</sup> The Zintl ion, which precipitated as an orange-red solid from the reaction mixture upon mixing the two reagents, was separated by suction filtration from the supernatant and identified by its diagnostic single broad resonance at -122.0 ppm in the  $^{31}\text{P}$  NMR spectrum<sup>38</sup> obtained by analyzing a solution of the precipitated solid in THF. Multinuclear NMR analysis of the supernatant revealed the formation of a major

Table 1. Summary of P–Sn Bond Distances, Sn–P–Sn Bond Angles, and  $^{31}\text{P}$  and  $^{119}\text{Sn}$  NMR Data for  $\text{R}^*\text{P}(\text{SnPh}_3)_2$  Derivatives

$\text{R}^*{}^a$	P–Sn [Å]	Sn–P–Sn [deg]	$^{31}\text{P}$ NMR ( $\delta$ , ppm)	$^{119}\text{Sn}$ NMR ( $\delta$ , ppm)
Na(crown)	2.439(1) 2.438(1)	101.07(5)	–367.2	–11
$(\text{XL})_2\text{In}$	2.4984(8) 2.4933(8)	103.55(3)	–309.9	–65.9
$(\text{Ph}_3\text{P})\text{Au}$	2.492(1) 2.502(1)	107.66(6)	–303.9	–44.1
$\text{SnPh}_3$	2.5068(6) 2.5082(6) 2.5108(6)	104.25(2) 103.04(2) 102.26(2)	–325.2	–69.2

<sup>a</sup> $\text{R}^* = \text{Na}(\text{benzo-15-crown-5})$ ,  $\text{SnPh}_3$ ,  $(\text{XL})_2\text{In}$  ( $\text{XL} = \text{S}(\text{CH}_2)_2\text{NMe}_2$ ), and  $(\text{Ph}_3\text{P})\text{Au}$ .

new species with resonances at –11.0 ppm in the  $^{119}\text{Sn}$  NMR spectrum, at –367.2 ppm in the  $^{31}\text{P}$  NMR spectrum, and a coupling constant of  $^1J_{^{119}\text{SnP}} = 1395$  Hz, as well as the presence of small amounts of unreacted  $\text{P}_4$ . To aid the purification and characterization of the new salt, the sodium cation was partially sequestered by addition of benzo-15-crown-5 to the supernatant, as described in the Experimental Section.

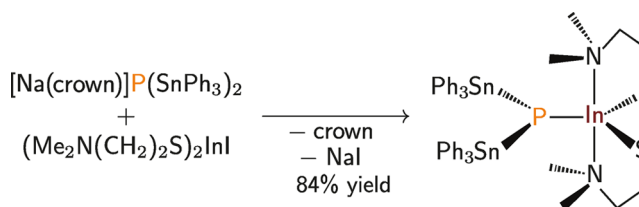
The synthesis of the monophosphide  $[\text{Na}(\text{benzo-15-crown-5})][\text{P}(\text{SnPh}_3)_2]$  salt in a one-pot reaction from white phosphorus is advantageous and constitutes, to our knowledge, the first report of direct  $\text{P}_4$  functionalization by a stannyl anion. Select aryl and silyl phosphides have been synthesized by direct activation of  $\text{P}_4$  with aryllithium and bulky alkali silanides, respectively.<sup>39,40</sup> In the case of aryl phosphides the steric bulk of the organolithium reagent determined the nuclearity of the aryl phosphide obtained. Thus, only one of the six P–P bonds of the  $\text{P}_4$  cage was cleaved with 2,4,6-tri-*tert*-butylphenyllithium,<sup>41</sup> whereas all six P–P bonds were cleaved with phenyllithium.<sup>42</sup> When bulky silyl nucleophiles  $[\text{M}][\text{Si}^t\text{Bu}_3]$ ,  $[\text{M}][\text{Si}^t\text{Bu}_2\text{Ph}]$ , and  $[\text{M}][\text{Si}(\text{SiMe}_3)_3]$  ( $\text{M} = \text{Li}, \text{Na}, \text{K}, \text{Cs}$ ) were used, the extent of fragmentation of the  $\text{P}_4$  cage increased with the number of silanide equivalents and solvent polarity.<sup>40,43–45</sup> For example, the 1:1 reaction of the hypersilyl salt  $[\text{K}(18\text{-crown-6})][\text{Si}(\text{SiMe}_3)_3]$  with  $\text{P}_4$  in toluene, led to formation of the disubstituted nortricyclic Zintl ion  $[\text{K}(18\text{-crown-6})]_2[\text{P}_7(\text{PR})(\text{R})]$  ( $\text{R} = \text{Si}(\text{SiMe}_3)_3$ ) in ca. 30% yield, ostensibly via dimerization of the putative  $[\text{RP}_4]^-$  anion.<sup>44</sup> In contrast, in the 2:1 reaction of supersilyl salt  $[\text{Na}][\text{Si}^t\text{Bu}_3]$  with  $\text{P}_4$  in THF or DME,  $[\text{Na}][\text{P}(\text{R}')-\text{P}=\text{P}(\text{R}')][\text{Na}]$  ( $\text{R}' = \text{Si}^t\text{Bu}_3$ ) formed quantitatively.<sup>43</sup> It is noteworthy that the complete fragmentation of the  $\text{P}_4$  cage to synthetically useful silyl monophosphides was negligible.

The monophosphide  $[\text{P}(\text{SnPh}_3)_2]^-$  anion has the potential to form homo- and heteroleptic tin phosphides by appropriate selection of a salt metathesis partner. Investigating this possibility, we first demonstrated that treatment of  $[\text{Na}(\text{benzo-15-crown-5})][\text{P}(\text{SnPh}_3)_2]$  with  $\text{ClSnPh}_3$  leads to the formation of the homoleptic phosphide  $\text{P}(\text{SnPh}_3)_3$ , isolated in 65% yield. The latter phosphide has been traditionally prepared using either  $\text{PH}_3$ <sup>46</sup> or  $\text{PCl}_3$ <sup>47</sup> as the phosphorus source, and more recently by effective  $[\text{SnPh}_3]$  radical addition to molecular phosphorus, in analogy with the phosphorus chlorination process.<sup>48</sup>

Seeking to prepare heteroleptic tin phosphides to serve as potential single-source precursors<sup>49</sup> to indium phosphide materials, we turned to the reported indium monoiodide  $(\text{XL})_2\text{InI}$ ,<sup>10</sup> which we expected to give rise to a molecule with a 1:1 ratio of In/P. Additionally, its thiolate XL units will potentially be removable subsequently as  $\text{Ph}_3\text{SnXL}$ .<sup>50</sup> The

indium phosphide  $(\text{XL})_2\text{InP}(\text{SnPh}_3)_2$  was obtained in 84% isolated yield as a monomeric species (see Scheme 2). Several indium diorganophosphides, including  $[\text{Cp}^*(\text{Cl})\text{InP}(\text{SiMe}_3)_2]_2$ , have been investigated previously as single-source precursors to indium phosphide particles.<sup>49,51</sup>

#### Scheme 2<sup>a</sup>



<sup>a</sup>The sodium phosphide salt  $[\text{Na}(\text{benzo-15-crown-5})][\text{P}(\text{SnPh}_3)_2]$  was used to prepare the indium phosphide  $(\text{XL})_2\text{InP}(\text{SnPh}_3)_2$ , isolated in 84% yield (crown = benzo-15-crown-5).

Additionally, the Zintl ion  $[\text{Na}_3][\text{P}_7]$ , formed as a coproduct in the synthesis of the monophosphide  $[\text{P}(\text{SnPh}_3)_2]^-$  anion, can be prepared selectively via an independent method that entails the treatment of a slurry of  $\text{P}_4$  with freshly prepared sodium naphthalenide in DME at 22 °C. The corresponding polyphosphides  $\text{P}_7\text{R}_3$  ( $\text{R} = \text{SiMe}_3, \text{SnPh}_3$ ) obtained by salt metathesis from this reaction were isolated in better than 65% yield. The traditional synthesis of the heptaphosphide  $[\text{Na}_3][\text{P}_7]$  entails harsher reaction conditions, either of refluxing white phosphorus and Na/K alloy in DME<sup>16</sup> or of heating the elements in a sealed and evacuated ampule at 770 K.<sup>52,53</sup>

Typically, the reaction of  $\text{P}_4$  with alkali metals gives rise to numerous products.<sup>53,54</sup> For example, in refluxing DME the reduction with alkali metals gives rise to a mixture of the polyphosphide ions  $\text{P}_7^{3-}$ ,  $\text{P}_9^{3-}$ ,  $\text{P}_{19}^{4-}$ ,  $\text{P}_{26}^{3-}$ ,  $\text{P}_{21}^{3-}$ ,  $\text{P}_{16}^{2-}$ , and even to *cyclo-P\_5*<sup>-</sup>, when 18-crown-6 is present.<sup>55–57</sup> In contrast, the reduction of  $\text{P}_4$  with Na/K naphthalenide in DME at low temperatures allows the isolation of  $[\text{Na}/\text{K}][\text{HP}_4]$  solutions, the  $[\text{HP}_4]^-$  anion being a key intermediate in the formation of higher-nuclearity polyphosphide anions.<sup>40,58</sup>

The solid-state structure of  $[\text{Na}(\text{benzo-15-crown-5})][\text{P}(\text{SnPh}_3)_2]$  is the first example of a monomeric bis(stannyl) monophosphide. The only other reported structure of a bis(stannyl) phosphide is that of  $\{\text{Li}(\text{THF})_2[\text{P}(\text{SnMe}_3)_2]\}_2$ , the latter having a structure that features two lithium bridges between the two phosphorus atoms of the dimeric unit.<sup>4</sup> The P–Sn interatomic distances in both  $[\text{Na}(\text{benzo-15-crown-5})][\text{P}(\text{SnPh}_3)_2]$ , of 2.439(1) and 2.438(1) Å, and  $\{\text{Li}(\text{THF})_2[\text{P}(\text{SnMe}_3)_2]\}_2$ , of 2.439(2) and 2.424(2) Å, fall right

between 2.51 and 2.32 Å, these being the values indicated for a P–Sn single and double bond, respectively.<sup>59</sup> This is suggestive of a bond order that is >1 between the electron-rich phosphorus and the tin atoms.

The cage phosphide  $P_4(SnMe_2)_6$ , obtained from  $P(SnMe_3)_3$  in the presence of small amounts of  $(ZnCl)_2Fe(CO)_4(THF)_2$ ,<sup>60</sup> provides the closest reported structural match to  $P(SnPh_3)_3$ . The P–Sn interatomic distances of 2.5068(6), 2.5082(6), and 2.5108(6) Å for  $P(SnPh_3)_3$ , and averaging 2.505 Å in  $P_4(SnMe_2)_6$ , are typical values for single P–Sn bonds. The pyramidalization at phosphorus in the two compounds is also similar, as measured by the sum of bond angles at phosphorus of 309.55(2)° in  $P(SnPh_3)_3$  and averaging 308° in  $P_4(SnMe_2)_6$ . Among the reported homoleptic stannyl monophosphides  $P(SnR''_3)_3$  ( $R'' = CH_3$ ,<sup>61</sup>  $n-C_4H_9$ ,<sup>62</sup>  $tert-C_4H_9$ ,<sup>63</sup>), the phosphide  $P(SnPh_3)_3$  appears to be the first one to be crystallographically characterized.<sup>36</sup>

Similar to the phosphide  $[Na(\text{benzo-15-crown-5})][P(SnPh_3)_2]$ , the indium phosphide  $(XL)_2InP(SnPh_3)_2$  is also monomeric (see Figure 3). Analogous indium phosphides

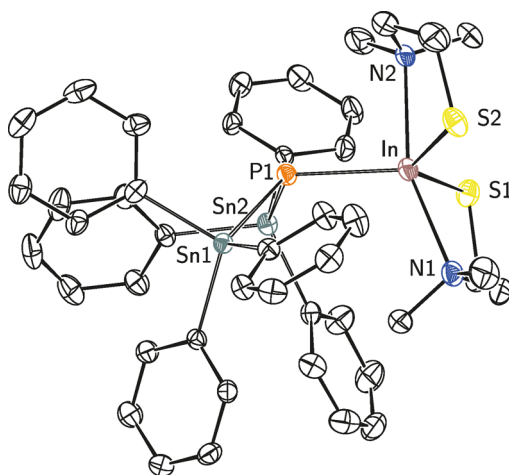


**Figure 3.** Solid-state molecular structure of  $(XL)_2InP(SnPh_3)_2$  with ellipsoids at the 50% probability level and rendered using PLATON.<sup>11</sup> Hydrogen atoms and the solvent molecule are omitted for clarity. Selected interatomic distances [Å] and angles [deg]: P1–Sn1 2.4984(8), P1–Sn2 2.4933(8), P1–In 2.5470(9), In–N1 2.451(6), In–S1 2.463(4), In–N2 2.465(8), In–S1 2.463(4), Sn1–P1–Sn2 103.55(3), Sn1–P1–In 119.71(3), Sn2–P1–In 105.21(3).

supported by less bulky ligands form oligomers, such as  $[Me_2InP(SnMe_3)_2]_3$ <sup>64</sup> or  $[Cp^*(Cl)InP(SiMe_3)_2]_2$ .<sup>51</sup> A lighter congener, the monomeric aluminum phosphide  $(2,6-Me_2Pip)_2AlP(SnMe_3)_2$ ,<sup>4</sup> (Pip = piperidine) is structurally similar to the indium phosphide  $(XL)_2InP(SnPh_3)_2$  as seen from the sum of angles at phosphorus of 328.47(3)° in  $(XL)_2InP(SnPh_3)_2$  and 326.32(5)° in  $(2,6-Me_2Pip)_2AlP(SnMe_3)_2$ , and the P–Sn interatomic distances of 2.4984(8) and 2.4933(8) Å in  $(XL)_2InP(SnPh_3)_2$  and of 2.479(1) and 2.478(1) Å in  $(2,6-Me_2Pip)_2AlP(SnMe_3)_2$ , consistent with a P–Sn single bond. The P–In bond distance of 2.5470(9) Å is slightly longer than 2.53 Å, the value expected for a P–In single bond.<sup>59</sup>

The monomeric gold phosphide  $(Ph_3P)AuP(SnPh_3)_2$  crystallizes in the triclinic space group  $P\bar{1}$  with four almost-identical molecules per asymmetric unit, one of which is discussed herein (see Figure 4). The structure is not remarkable with respect to the metrical parameters; indeed, these compare

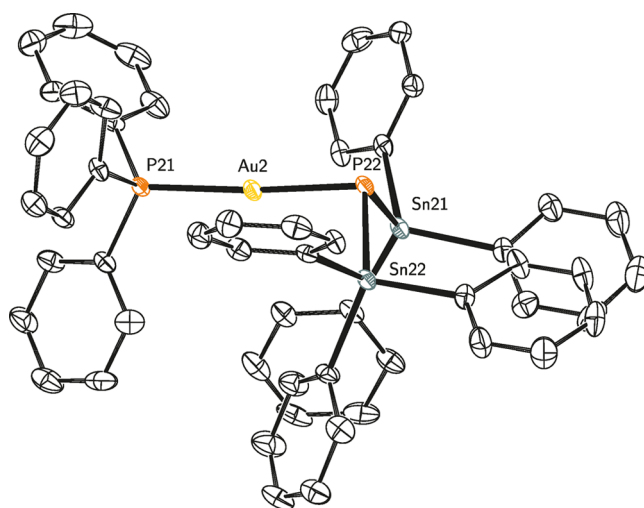


**Figure 4.** Solid-state molecular structure of  $(Ph_3P)AuP(SnPh_3)_2$  with ellipsoids at the 50% probability level and rendered using PLATON.<sup>11</sup> The other three molecules of  $(Ph_3P)AuP(SnPh_3)_2$  present in the asymmetric unit and hydrogen atoms are omitted for clarity. Selected interatomic distances [Å] and angles [deg]: P21–Au2 2.293(1), Au2–P22 2.320(1), P22–Sn22 2.492(1), P22–Sn21 2.502(1), Sn22–P22–Sn21 107.66(6), Au2–P22–Sn22 95.83(6), P21–Au2–P22 175.18(6).

well to those reported together with complete structural data for gold phosphane and phosphanido complexes.<sup>65,66</sup> The arrangement of the two phosphorus atoms is almost linear around the Au(I) center, with an angle of P21–Au–P22 of 175.18(6)°. The interatomic distance of 2.320(1) Å between P22, the X-type phosphorus ligand,<sup>9</sup> and the gold center is only slightly shorter than 2.35 Å, the calculated value for a P–Au single bond.<sup>59</sup> The P21–Au2 interatomic distance of 2.293(1) Å is typical for a gold–phosphine bond.<sup>67</sup>

In accordance with general trends observed for <sup>31</sup>P NMR shifts,<sup>68</sup> the electronegativity of the R\* ( $R^* = Na(\text{benzo-15-crown-5})$ ,  $SnPh_3$ ,  $In(XL)_2$ ,  $(Ph_3P)Au$ ) substituent on  $R^*P(SnPh_3)_2$  phosphide correlates inversely with an upfield shift in the observed <sup>31</sup>P NMR resonances (see Table 1).

**NBO Study of Dative versus Shared Electron-Pair Au–P Bonding in the Same Molecule.** It is interesting to note that  $(Ph_3P)AuP(SnPh_3)_2$  is an example of a gold(I) compound that offers an intramolecular comparison of two different bond types. The covalent single bond between gold and the phosphanido ligand should have a distance close to the sum of covalent radii for the two elements (1.24 + 1.11 = 2.35 Å),<sup>59</sup> and this is found experimentally to be the case (2.320(1) Å). On the other hand, since dative or donor–acceptor bonds are generally weaker than shared electron-pair bonds,<sup>69</sup> there is also the expectation that the interatomic distance Au–P(phosphine) should be longer than that to the phosphanido ligand, but experimentally we find that it is marginally shorter: 2.293(1) Å. That this is not an anomaly is suggested by the corresponding distances calculated for the simple model system  $H_3P-Au-PH_2$  using MP2 theory: 2.30, 2.26 Å; here too, the gold–phosphine distance is shorter by ca. 0.04 Å than is the gold–phosphanido distance. A similar circumstance was reported also for the only other structurally characterized phosphine/phosphanido system.<sup>65</sup> The basis for the closeness in the interatomic distances displayed for these two very different bond types (covalent versus dative) is that the hybrid orbital used by phosphorus for the dative bond very rich in s character

(NBO analysis shows the phosphine lone pair to be 52% s, 48% p), while for the shared electron-pair bond it is much less so (15% s, 85% p) (Figure 5). Keep in mind that assignment of

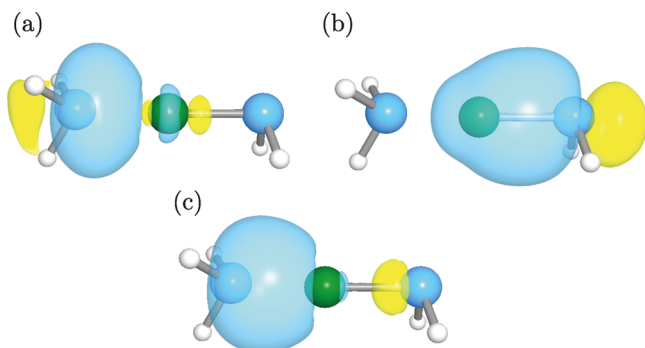


**Figure 5.** (a) The natural bond orbitals (NBOs) corresponding to the dative bond phosphine–gold interaction, (b) the covalent phosphanido–gold bond, and (c) the natural localized molecular orbital (NLMO) corresponding to the phosphine lone pair donation into the Au–P(phosphanide)  $\sigma^*$  orbital in the model complex  $\text{H}_3\text{P}:\text{Au}-\text{PH}_2$ , built and optimized at the MP2 level of theory<sup>22,71</sup> and visualized using NBOView 2.0.<sup>72</sup>

the triphenylphosphine ligand as a dative ligand is not arbitrary: its structural parameters in the complex are nearly the same as in the free ligand.<sup>70</sup> Furthermore, natural resonance theory (NRT) analysis shows that  $\text{H}_3\text{P}:\text{Au}-\text{PH}_2$  is the dominant resonance structure for the model. This makes sense given that the  $d^{10}$  gold center has only its 6s orbital available for bonding, such that any gold–phosphine bonding must come at the expense of gold–phosphanide bonding. Phosphine lone-pair donation into the Au–P(phosphanide)  $\sigma^*$  orbital indeed is associated with a large second-order perturbation theory stabilization energy ( $\Delta E_{i \rightarrow j}^{(2)}$ ) of ca. 168 kcal/mol. The natural valence of gold in the model system is 1.0, meaning that the gold forms a total of one electron-pair bond. The natural valence for the phosphanide phosphorus is 2.7, reduced from 3 by the same amount that the natural valence for the phosphine phosphorus (3.3) exceeds it. These computational descriptors for the model system at the MP2 level, where this model has previously been considered in a study on auriphilic interactions,<sup>73</sup> are well reproduced at the B3LYP level of theory.

**Solid-State NMR Analysis of  $(\text{XL})_2\text{InP}(\text{SnPh}_3)_2$ .** To further investigate the chemical bonding in  $(\text{XL})_2\text{InP}(\text{SnPh}_3)_2$ , we recorded solid-state  $^{31}\text{P}$  and  $^{13}\text{C}$  NMR spectra at 14.0 T. As seen from Figure 6a, the  $^{31}\text{P}$  CP/MAS NMR spectrum of  $(\text{XL})_2\text{InP}(\text{SnPh}_3)_2$  exhibits a broad peak centered at  $-304$  ppm. This  $^{31}\text{P}$  isotropic chemical shift is in good agreement with that measured in solution,  $\delta(^{31}\text{P}) = -309.9$  ppm, suggesting that the molecular structures of  $(\text{XL})_2\text{InP}(\text{SnPh}_3)_2$  in the solid and solution states are essentially the same. This was further confirmed by the excellent agreement between the  $^{13}\text{C}$  chemical shifts observed in the two phases (data are provided in the Supporting Information). Furthermore, the sharp peaks observed in the solid-state  $^{13}\text{C}$  NMR spectrum of  $(\text{XL})_2\text{InP}(\text{SnPh}_3)_2$  suggest that the solid sample used in our study is highly crystalline. It is important to note that the  $^{31}\text{P}$  NMR peak is rather broad, with a full-width at the half-height (fwhh) of ca. 2800 Hz, and exhibits an asymmetrical line shape. In general, such features in MAS NMR spectra of spin-1/2 nuclei are caused by the presence of a neighboring quadrupolar

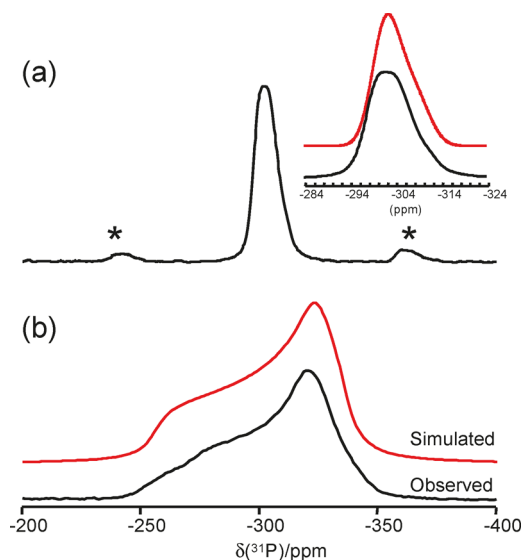


**Figure 6.** Solid-state (a) MAS and (b) static  $^{31}\text{P}$  NMR spectra of  $(\text{XL})_2\text{InP}(\text{SnPh}_3)_2$  recorded at 14.0 T. Spinning sidebands (ssb) are marked with \*. (inset) The (black) observed and (red) simulated line shape for the central band.

( $I > 1/2$ ) nucleus. In the present case, both residual dipolar coupling and indirect spin–spin ( $J$ ) coupling between  $^{31}\text{P}$  and  $^{115}\text{In}$  ( $I = 9/2$ , natural abundance 95.72%) nuclei contribute to the observed line shape. To properly analyze the observed line shape, it is necessary to know the magnitude of the  $^{115}\text{In}$  quadrupole coupling constant  $C_Q(^{115}\text{In})$ . However, our attempts to directly observe a solid-state  $^{115}\text{In}$  NMR signal for  $(\text{XL})_2\text{InP}(\text{SnPh}_3)_2$  at 14.0 T were unsuccessful, suggesting that the value of  $C_Q(^{115}\text{In})$  in  $(\text{XL})_2\text{InP}(\text{SnPh}_3)_2$  must be very large. Indeed, the ADF calculation predicts that  $C_Q(^{115}\text{In}) = 255$  MHz in  $(\text{XL})_2\text{InP}(\text{SnPh}_3)_2$ ; see Table 2. Recently,

**Table 2.** Experimental and Computed NMR Parameters for  $(\text{XL})_2\text{InP}(\text{SnPh}_3)_2$

	exp.	ADF-ZORA
$\delta_{\text{iso}}(^{31}\text{P})/\text{ppm}$	$-304^a$	$-311$
$\delta_{11}(^{31}\text{P})/\text{ppm}$	$-255^a$	$-286$
$\delta_{22}(^{31}\text{P})/\text{ppm}$	$-322^a$	$-312$
$\delta_{33}(^{31}\text{P})/\text{ppm}$	$-335^a$	$-333$
$\Omega/\text{ppm}$	$80^a$	$47$
$^1J(^{31}\text{P}, ^{115}\text{In})/\text{Hz}$	$250^a$	$361$
$^1J(^{31}\text{P}, ^{117/119}\text{Sn})/\text{Hz}$	$993^b$	$808$
$\delta_{\text{iso}}(^{115}\text{In})/\text{ppm}$	ND <sup>d</sup>	$248^c$
$C_Q(^{115}\text{In})/\text{MHz}$	ND <sup>d</sup>	$255$
$\eta_Q(^{115}\text{In})$	ND <sup>d</sup>	$0.08$

<sup>a</sup>Measured by solid-state  $^{31}\text{P}$  NMR. <sup>b</sup>Measured by solution  $^{31}\text{P}$  NMR. <sup>c</sup>Computed  $^{115}\text{In}$  shielding constant was converted to the  $^{115}\text{In}$  chemical shift with reference to 0.1 M  $\text{In}(\text{NO}_3)_3$  (aq) using the following equation:  $\delta_{\text{iso}}(^{115}\text{In}) = 3840 - \sigma_{\text{iso}}(^{115}\text{In})$ . <sup>d</sup>Not determined.

Wasylishen and co-workers<sup>74,75</sup> reported solid-state  $^{115}\text{In}$  NMR spectra of several indium(III) compounds. We note that the largest  $C_Q(^{115}\text{In})$  value for which they were able to record a solid-state  $^{115}\text{In}$  NMR spectrum at an ultrahigh magnetic field, 21 T, is about 200 MHz. At 14.0 T, a  $C_Q(^{115}\text{In})$  value of 255 MHz produces a static  $^{115}\text{In}$  NMR spectrum of 3.4 MHz wide. The very large  $C_Q(^{115}\text{In})$  value in  $(\text{XL})_2\text{InP}(\text{SnPh}_3)_2$  also explains why  $^1J(^{31}\text{P}, ^{115}\text{In})$  is completely self-

decoupled in the solution  $^{31}\text{P}$  NMR spectrum. If we assume a  $C_Q(^{115}\text{In})$  value of 255 MHz, the observed  $^{31}\text{P}$  NMR line shape can be qualitatively reproduced by simulation from which we obtained an estimate for  $^1J(^{31}\text{P}, ^{115}\text{In})$ , 250 Hz; see Figure 6a. To obtain the full  $^{31}\text{P}$  chemical shift tensor for  $(\text{XL})_2\text{InP}(\text{SnPh}_3)_2$ , we recorded a solid-state  $^{31}\text{P}$  NMR spectrum under the static condition, as shown in Figure 6b. The experimental  $^{31}\text{P}$  chemical shift tensor parameters are listed in Table 2, together with the ADF computational results. In general, the experimental NMR parameters are qualitatively reproduced by ADF computations.

The  $^{31}\text{P}$  chemical shift observed for  $(\text{XL})_2\text{InP}(\text{SnPh}_3)_2$  is among the most negative (most shielded)  $^{31}\text{P}$  chemical shifts reported for phosphorus compounds, for example,  $\text{PH}_3(\text{g})$ ,  $-271.58$  ppm; $^{25}$   $\text{AsP}_3(\text{s})$ ,  $-413$  ppm; $^{76}$   $\text{P}_4(\text{g})$ ,  $-551.5$  ppm. $^{77}$  The  $^{31}\text{P}$  chemical shift tensor observed in  $(\text{XL})_2\text{InP}(\text{SnPh}_3)_2$  is also strikingly similar to that for  $\text{PH}_3(\text{g})$ ,  $\delta_{11} = -228.5$  ppm,  $\delta_{22} = \delta_{33} = -293.0$  ppm. $^{78,79}$  Both  $(\text{XL})_2\text{InP}(\text{SnPh}_3)_2$  and  $\text{PH}_3$  exhibit rather small  $^{31}\text{P}$  chemical shift anisotropy, which is generally measured by the span of the chemical shift tensor ( $\Omega = \delta_{11} - \delta_{33}$ ). For  $(\text{XL})_2\text{InP}(\text{SnPh}_3)_2$ ,  $\Omega = 80$  ppm, which compares to  $\Omega = 64.5$  ppm found for  $\text{PH}_3(\text{g})$ . The nearly axially symmetric  $^{31}\text{P}$  chemical shift tensor ( $\delta_{22} \approx \delta_{33}$ ) observed for  $(\text{XL})_2\text{InP}(\text{SnPh}_3)_2$  also suggests that the three chemical bonds around the P atom are similar. Indeed, the crystal structure of  $(\text{XL})_2\text{InP}(\text{SnPh}_3)_2$  shows that the In–P1 and Sn1–P1 bond lengths are 2.5470(9) and 2.4984(8) Å, respectively. The trigonal pyramidal core of  $(\text{XL})_2\text{InP}(\text{SnPh}_3)_2$  is slightly “flatter” than that in  $\text{PH}_3$ : the In–P–Sn1, In–P–Sn2, and Sn1–P–Sn2 angles range from 103.55(3) to 119.71(3)°, these being larger than those in  $\text{PH}_3$ : 93°. It is interesting to note that the value of  $^1J(^{31}\text{P}, ^{115}\text{In})$  in  $(\text{XL})_2\text{InP}(\text{SnPh}_3)_2$ , 250 Hz, is considerably smaller than those reported by Wasylishen and co-workers $^{75,80}$  for triarylphosphine indium(III) trihalide adducts, for which the  $^1J(^{31}\text{P}, ^{115}\text{In})$  values are in a range between 550 and 2500 Hz. This difference can be understood on the basis of the nature of indium–phosphorus bonding in these compounds. In In(III)–phosphine adducts, the nonbonding lone pair orbital from the phosphorus atom participates in the indium–phosphorus bonding. In  $(\text{XL})_2\text{InP}(\text{SnPh}_3)_2$ , however, it is one of the three  $\sigma$  bonding orbitals on the phosphorus atom that contributes to the indium–phosphorus bond. As the lone-pair orbital on the phosphorus atom is known to have significantly more s character (from the phosphorus 3s orbital) than the other three  $\sigma$ -bonding orbitals, it is not surprising that the  $^1J(^{31}\text{P}, ^{115}\text{In})$  couplings in In(III)–phosphine adducts are generally larger than that seen in  $(\text{XL})_2\text{InP}(\text{SnPh}_3)_2$ . $^{68,81}$  Similarly, the  $^1J(^{31}\text{P}, ^{117/119}\text{Sn})$  value of 993 Hz in  $(\text{XL})_2\text{InP}(\text{SnPh}_3)_2$ , while larger than that of  $^1J(^{31}\text{P}, ^{115}\text{In})$  as a consequence of the high  $\gamma(^{117/119}\text{Sn})$  values, is still much smaller than the typical values reported for Sn(IV)–phosphine complexes, ca. 2300 Hz. $^{82,83}$

#### 4. CONCLUSIONS

With this work we introduce a facile synthesis of the new phosphide reagent,  $[\text{Na}(\text{benzo-15-crown-5})][\text{P}(\text{SnPh}_3)_2]$ . This monoposphide serves as a precursor to homo- and heteroleptic phosphides  $\text{P}(\text{SnPh}_3)_3$  or  $(\text{XL})_2\text{InP}(\text{SnPh}_3)_2$ , foreshadowing potential applications to the synthesis of other phosphides, especially those that may be targeted as potential precursors to III–V semiconductor materials. $^{84}$

#### ■ ASSOCIATED CONTENT

##### ■ Supporting Information

Additional synthetic and spectroscopic details, including NMR spectra and crystallographic tables, may be found in the Supporting Information document accompanying this manuscript. This material is available free of charge via the Internet at <http://pubs.acs.org>.

#### ■ AUTHOR INFORMATION

##### Corresponding Authors

\*E-mail: [gang.wu@chem.queensu.ca](mailto:gang.wu@chem.queensu.ca) (G.W.).

\*E-mail: [ccummins@mit.edu](mailto:ccummins@mit.edu) (C.C.C.).

\*E-mail: [avelian@mit.edu](mailto:avelian@mit.edu) (A.V.).

##### Notes

The authors declare no competing financial interest.

#### ■ ACKNOWLEDGMENTS

This material is based upon work supported by the National Science Foundation under CHE-1111357. C.H. thanks the China Scholarship Council for their financial support. Runyu Tan is thanked for crystallographic assistance. Thermphos International is thanked for a gift of white phosphorus. G.W. thanks NSERC of Canada for financial support.

#### ■ REFERENCES

- Rösch, W.; Vogelbacher, U.; Allspach, T.; Regitz, M. J. *Organomet. Chem.* **1986**, *306*, 39–53.
- Weber, L.; Meine, G. *Chem. Ber.* **1987**, *120*, 457–459.
- Antcliff, K. L.; Baker, R. J.; Jones, C.; Murphy, D. M.; Rose, R. P. *Inorg. Chem.* **2005**, *44*, 2098–2105.
- Habereder, T.; Nöth, H.; Paine, R. T. *Eur. J. Inorg. Chem.* **2007**, *2007*, 4298–4305.
- Ionkin, A. S.; Marshall, W. J.; Fish, B. M.; Schiffhauer, M. F.; McEwen, C. N. *Chem. Commun.* **2008**, 5432–5434.
- Fritz, G.; Scheer, P. *Chem. Rev.* **2000**, *100*, 3341–3402.
- Becker, G.; Schmidt, H.; Uhl, G.; Uhl, W.; Regitz, M.; Rösch, W.; Vogelbacher, U.-J. *Inorg. Synth.* **1990**, *27*, 243–249.
- Scott, N. D.; Walker, J. F.; Hansley, V. L. *J. Am. Chem. Soc.* **1936**, *58*, 2442–2444.
- Green, M. L. H. *J. Organomet. Chem.* **1995**, *500*, 127–148.
- Briand, G. G.; Cooper, B. F. T.; MacDonald, D. B. S.; Martin, C. D.; Schatte, G. *Inorg. Chem.* **2006**, *45*, 8423–8429.
- Spek, A. L. *J. Appl. Crystallogr.* **2003**, *36*, 7–13.
- Eichele, K. *WSolidsI*, Version 1.20.21; Universität Tübingen: Tübingen, Germany, 2013.
- Blake, D.; Coates, G. E.; Tate, J. M. *J. Chem. Soc.* **1961**, 618–622.
- (a) Fritz, G.; Hoppe, K.; Hönle, W.; Weber, D.; Mujica, C.; Manriquez, V.; Schnering, H. *J. Organomet. Chem.* **1983**, *249*, 63–80. (b) Knapp, C. M.; Large, J. S.; Rees, N. H.; Goicoechea, J. M. *Dalton Trans.* **2011**, *40*, 735–745.
- Mujica, C.; Weber, D.; von Schnering, H. G. *Z. Naturforsch., B: Anorg. Chem., Org. Chem.* **1986**, *41b*, 991–999.
- Fritz, G.; Hölderich, W. *Naturwissenschaften* **1975**, *62*, 573–575.
- te Velde, G.; Bickelhaupt, F. M.; Baerends, E. J.; Guerra, C. F.; van Gisbergen, S. J. A.; Snijders, J. G.; Ziegler, T. *J. Comput. Chem.* **2001**, *22*, 931–967.
- Vosko, S. H.; Wilk, L.; Nusair, M. *Can. J. Phys.* **1980**, *58*, 1200–1211.
- Perdew, J. P.; Burke, K.; Ernzerhof, M. *Phys. Rev. Lett.* **1996**, *77*, 3865–3868.
- (a) van Lenthe, E.; Baerends, E. J.; Snijders, J. G. *J. Chem. Phys.* **1993**, *99*, 4597–4610. (b) van Lenthe, E.; Baerends, E. J.; Snijders, J. G. *J. Chem. Phys.* **1994**, *101*, 9783–9792. (c) van Lenthe, E.; Snijders, J. G.; Baerends, E. J. *J. Chem. Phys.* **1996**, *105*, 6505–6516. (d) van



- Lenthe, E.; van Leeuwen, R.; Baerends, E. J.; Snijders, J. G. *Int. J. Quantum Chem.* **1996**, *57*, 281–293.
- (21) Jameson, C. J.; De Dios, A.; Keith Jameson, A. *Chem. Phys. Lett.* **1990**, *167*, 575–582.
- (22) Schaftenaar, G.; Noordik, J. J. *Comput.-Aided Mol. Des.* **2000**, *14*, 123–134.
- (23) (a) Head-Gordon, M.; Pople, J. A.; Frisch, M. J. *Chem. Phys. Lett.* **1988**, *153*, 503–506. (b) Neese, F.; Petrenko, T.; Ganyushin, D.; Olbrich, G. *Coord. Chem. Rev.* **2007**, *251*, 288–327. (c) Ganyushin, D.; Neese, F. *J. Chem. Phys.* **2008**, *128*, 114117.
- (24) Neese, F. *ORCA—an ab initio, Density Functional and Semiempirical Program Package*, Version 3.0.1; University of Bonn: Bonn, Germany, 2013.
- (25) Lee, C.; Yang, W.; Parr, R. G. *Phys. Rev. B* **1988**, *37*, 785–789.
- (26) Perdew, Y.; Wang, J. P. *Phys. Rev. B: Condens. Matter Mater. Phys.* **1992**, *45*, 13244–13249.
- (27) (a) Becke, A. D. *Phys. Rev. A* **1988**, *38*, 3098–3100. (b) Perdew, J. P. *Phys. Rev. B: Condens. Matter Mater. Phys.* **1986**, *33*, 8822–8824.
- (28) Schaefer, A.; Horn, H.; Ahlrichs, R. *J. Chem. Phys.* **1992**, *97*, 2571–2577.
- (29) (a) Glendening, E. D.; Badenhop, J. K.; Reed, A. E.; Carpenter, J. E.; Bohmann, J. A.; Morales, C. M.; Weinhold, F. *NBO 5.0*; Theoretical Chemistry Institute, University of Wisconsin: Madison, WI, 2001. (b) Weinhold, F.; Landis, C. R. *Chem. Ed. Res. Pract. (CERP; special “Structural Concepts” issue)* **2001**, *2*, 91–104. (c) Foster, J. P.; Weinhold, F. *J. Am. Chem. Soc.* **1980**, *102*, 7211–7218.
- (30) (a) Glendening, E. D.; Weinhold, F. *J. Comput. Chem.* **1998**, *19*, 593–609. (b) Glendening, E. D.; Badenhop, J. K.; Weinhold, F. *J. Comput. Chem.* **1998**, *19*, 628–646.
- (31) Sheldrick, G. M. *SHELXTL*; Bruker AXS, Inc.: Madison, WI, 2005–2011.
- (32) Sheldrick, G. M. *Acta Crystallogr., Sect. A: Found. Crystallogr.* **1990**, *46*, 467–473.
- (33) Sheldrick, G. M. *Acta Crystallogr., Sect. A* **2008**, *64*, 112–122.
- (34) Sheldrick, G. M. *SHELXL-97*, Program for Crystal Structure Determination; University of Gottingen: Gottingen, Germany, 1997.
- (35) Müller, P.; Herbst-Irmer, R.; Spek, A. L.; Schneider, T. R.; Sawaya, M. R. *Crystal Structure Refinement: A Crystallographer's Guide to SHELXL*; IUCr Texts on Crystallography; Oxford University Press: Oxford, U.K., 2006.
- (36) These data can be obtained free of charge from The Cambridge Crystallographic Data Centre. [http://www.ccdc.cam.ac.uk/data\\_request/cif](http://www.ccdc.cam.ac.uk/data_request/cif).
- (37) Baudler, M.; Ternberger, H.; Faber, W.; Hahn, J. *Z. Naturforsch., Teil B* **1979**, *34*, 1690.
- (38) Manriquez, V.; Hönl, W.; von Schnering, H. G. *Z. Anorg. Allg. Chem.* **1986**, *539*, 95–109.
- (39) Engel, R. *Synthesis of Carbon Phosphorus Bonds*, 2nd ed.; CRC Press: Boca Raton, FL, 2004.
- (40) Scheer, M.; Balazs, G.; Seitz, A. *Chem. Rev.* **2010**, *110*, 4236–4256.
- (41) Riedel, R.; Hausen, H.-D.; Fluck, E. *Angew. Chem., Int. Ed.* **1985**, *24*, 1056–1057.
- (42) Rauhut, M. M.; Semsel, A. M. *J. Org. Chem.* **1963**, *28*, 473–477.
- (43) Wiberg, N.; Wörner, A.; Karaghiosoff, K.; Fenske, D. *Chem. Ber.* **1997**, *130*, 135–140.
- (44) Chan, W. T. K.; García, F.; Hopkins, A. D.; Martin, L. C.; McPartlin, M.; Wright, D. S. *Angew. Chem., Int. Ed.* **2007**, *46*, 3084–3086.
- (45) (a) Lerner, H.-W.; Bolte, M.; Karaghiosoff, K.; Wagner, M. *Organometallics* **2004**, *23*, 6073–6076. (b) Lerner, H.-W.; Margraf, G.; Kaufmann, L.; Bats, J. W.; Bolte, M.; Wagner, M. *Eur. J. Inorg. Chem.* **2005**, 1932–1939. (c) Lorbach, A.; Nadj, A.; Tillmann, S.; Dornhaus, F.; Schödel, F.; Sängler, I.; Margraf, G.; Bats, J. W.; Bolte, M.; Holthausen, M. C.; Wagner, M.; Lerner, H.-W. *Inorg. Chem.* **2008**, *48*, 1005–1017.
- (46) Schumann, H.; Schwabe, P.; Schmidt, M. *Inorg. Nucl. Chem. Lett.* **1966**, *2*, 309–310.
- (47) (a) Schumann, H.; Köpf, H.; Schmidt, M. *Chem. Ber.* **1964**, *97*, 2395–2399. (b) Schumann, H.; Schwabe, P.; Stelzer, O. *Chem. Ber.* **1969**, *102*, 2900–2913.
- (48) Cossairt, B. M.; Cummins, C. C. *New J. Chem.* **2010**, *34*, 1533–1536.
- (49) Green, M.; O'Brien, P. J. *Mater. Chem.* **2004**, *14*, 629–636.
- (50) Schumann, H.; Schumann-Ruidisch, I.; Schmidt, M. Chapter 6. In *Chemistry of Tin*; Smith, P. J., Ed.; Blackie: London; New York, 1998; pp 297–508.
- (51) (a) Douglas, T.; Theopold, K. H. *Inorg. Chem.* **1991**, *30*, 594–596. (b) Green, M. *Curr. Opin. Solid State Mater. Sci.* **2002**, *6*, 355–363. (c) Wells, R. L.; Pitt, C. G.; McPhail, A. T.; Purdy, A. P.; Shafieezad, S.; Hallock, R. B. *Chem. Mater.* **1989**, *1*, 4–6. (d) Healy, M. D.; Laibinis, P. E.; Stupik, P. D.; Barron, A. R. *J. Chem. Soc., Chem. Commun.* **1989**, 359–360.
- (52) Santandrea, R. P.; Mensing, C.; Von Schnering, H. G. *Thermochim. Acta* **1986**, *98*, 301–311.
- (53) Von Schnering, H. G.; Hönl, W. *Chem. Rev.* **1988**, *88*, 243–273.
- (54) Baudler, M. *Angew. Chem., Int. Ed. Engl.* **1987**, *26*, 419–441.
- (55) Baudler, M.; Düster, D.; Germeshausen, J. *Z. Anorg. Allg. Chem.* **1986**, *534*, 19–26.
- (56) Baudler, M.; Akpapoglou, S.; Ouzounis, D.; Wasgestian, F.; Meinigke, B.; Budzikiewicz, H.; Münster, H. *Angew. Chem., Int. Ed.* **1988**, *27*, 280–281.
- (57) Milyukov, V.; Kataev, A.; Sinyashin, O.; Hey-Hawkins, E. *Russ. Chem. B.* **2006**, *55*, 1297–1299.
- (58) Baudler, M.; Adamek, C.; Opiela, S.; Budzikiewicz, H.; Ouzounis, D. *Angew. Chem., Int. Ed. Engl.* **1988**, *27*, 1059–1061.
- (59) Pyykkö, P.; Atsumi, M. *Chem.—Eur. J.* **2009**, *15*, 12770–12779.
- (60) Fuhr, O.; Fenske, D. *Z. Anorg. Allg. Chem.* **2004**, *630*, 244–246.
- (61) Schumann, H.; Rösch, L. *Chem. Ber.* **1974**, *107*, 854–868.
- (62) Ebsworth, E.; Hutchison, D.; Macdonald, E.; Rankin, D. *Inorg. Nucl. Chem. Lett.* **1981**, *17*, 19–21.
- (63) Hänssgen, D.; Aldenhoven, H.; Nieger, M. *J. Organomet. Chem.* **1989**, *375*, C9–C12.
- (64) Schaller, A.; Hausen, H.-D.; Schwarz, W.; Heckmann, G.; Weidlein, J. *Z. Anorg. Allg. Chem.* **2000**, *626*, 1047–1058.
- (65) Gómez-Ruiz, S.; Wolf, R.; Bauer, S.; Bittig, H.; Schisler, A.; Lönnecke, P.; Hey-Hawkins, E. *Chem.—Eur. J.* **2008**, *14*, 4511–4520.
- (66) Stefanescu, D. M.; Yuen, H. F.; Glueck, D. S.; Golen, J. A.; Rheingold, A. L. *Angew. Chem., Int. Ed.* **2003**, *42*, 1046–1048.
- (67) A Cambridge Structural Database Search for gold-phosphine distances returned 3813 hits, with an average value for the bond distance of 2.28 Å.
- (68) Kühl, O. *Phosphorus-31 NMR Spectroscopy: a Concise Introduction for the Synthetic Organic and Organometallic Chemist*; Springer: Berlin, Germany, 2008.
- (69) Haaland, A. *Angew. Chem., Int. Ed. Engl.* **1989**, *28*, 992–1007.
- (70) Dunne, B. J.; Orpen, A. G. *Acta Crystallogr., Sect. C: Cryst. Struct. Commun.* **1991**, *47*, 345–347.
- (71) Neese, F. *ORCA—an ab initio, Density Functional and Semiempirical Program Package*, Version 2.8.0; University of Bonn: Bonn, Germany, 2009.
- (72) NBOView 2.0: NBO Orbital Graphics Plotter (C) Copyright 2013 by the Board of Regents of the University of Wisconsin System.
- (73) Pyykkö, P.; Tamm, T. *Organometallics* **1998**, *17*, 4842–4852.
- (74) Chen, F.; Ma, G.; Cavell, R. G.; Terskikh, V. V.; Wasylishen, R. E. *Chem. Commun.* **2008**, 5933–5935.
- (75) Chen, F.; Ma, G.; Bernard, G. M.; Cavell, R. G.; McDonald, R.; Ferguson, M. J.; Wasylishen, R. E. *J. Am. Chem. Soc.* **2010**, *132*, 5479–5493.
- (76) (a) Cossairt, B. M.; Diawara, M.-C.; Cummins, C. C. *Science* **2009**, *323*, 602–602. (b) Cossairt, B. M.; Cummins, C. C.; Head, A. R.; Lichtenberger, D. L.; Berger, R. J. F.; Hayes, S. A.; Mitzel, N. W.; Wu, G. *J. Am. Chem. Soc.* **2010**, *132*, 8459–8465.
- (77) Heckmann, G.; Fluck, E. *Mol. Phys.* **1972**, *23*, 175–183.
- (78) Jameson, C. J.; de Dios, A. C.; Jameson, A. K. *J. Chem. Phys.* **1991**, *95*, 9042–9053.

- (79) Gierke, T. D.; Flygare, W. H. *J. Am. Chem. Soc.* **1972**, *94*, 7277–7283.
- (80) Wasylshen, R. E.; Wright, K. C.; Eichele, K.; Cameron, T. S. *Inorg. Chem.* **1994**, *33*, 407–408.
- (81) Allen, D. W.; Taylor, B. F. *J. Chem. Soc., Dalton Trans.* **1982**, 51–54.
- (82) Malone, J.; Mann, B. *Inorg. Nucl. Chem. Lett.* **1972**, *8*, 819–821.
- (83) Yamasaki, A.; Fluck, E. *Z. Anorg. Allg. Chem.* **1973**, *396*, 297–302.
- (84) (a) Harris, D. K.; Bawendi, M. G. *J. Am. Chem. Soc.* **2012**, *134*, 20211–20213. (b) Buhro, W. E. *Polyhedron* **1994**, *13*, 1131–1148.